

## Compartment Analysis of Plant Cells by Means of Turgor Pressure Relaxation: II. Experimental Results on *Chara corallina*

Stephan Wendler<sup>†</sup> and Ulrich Zimmermann<sup>‡</sup>

<sup>†</sup>Arbeitsgruppe Membranforschung am Institut für Medizin der Kernforschungsanlage Jülich, 5170 Jülich, Federal Republic of Germany and <sup>‡</sup>Lehrstuhl für Biotechnologie der Universität Würzburg, 8700 Würzburg, Federal Republic of Germany

**Summary.** The three-compartment model (paper I) described turgor pressure relaxations as a sum of two exponential functions. The predicted shape of the curves could be confirmed in *Chara corallina* by improving the recording and processing of data. An evaluation on the basis of the three-compartment model provided values for the hydraulic conductivity of the plasmalemma of  $Lp_p = 2 \times 10^{-5}$  to  $4 \times 10^{-5}$  cm sec<sup>-1</sup> bar<sup>-1</sup> and of  $Lp_t = 3 \times 10^{-5}$  to  $1 \times 10^{-4}$  cm sec<sup>-1</sup> bar<sup>-1</sup> for the tonoplast (assuming the area to be 90% of the plasmalemma area). The mean proportion of the total volume occupied by the cytoplasm was calculated to be 9%. This value is consistent with the concept of a highly vacuolated cell. Other explanations for the biphasic relaxation curves are discussed.

**Key Words** *Chara corallina* · turgor pressure · relaxation · tonoplast · plasmalemma · cytoplasmic volume · hydraulic conductivity

### Introduction

In the preceding paper, we have demonstrated that, in principle, the hydraulic conductivities of both the plasmalemma and the tonoplast can be measured simultaneously without destroying the integrity of the plant cell. If the compartmentation of the cell into cytoplasm and vacuole is taken into account in the theoretical calculation of a pressure relaxation, the time course of turgor-pressure relaxation is described by the superposition of two exponential functions (paper I). The amplitudes and exponents of the relaxation curve are determined by a combination of the cell parameters such as the hydraulic conductivities of the membranes, the elasticity of the cell wall, the turgor pressure and the osmotic pressure due to solutes.

In this communication, we will show that the fresh-water alga *Chara corallina* exhibits turgor pressure relaxations consisting of two components which can be interpreted in terms of the three-compartment model introduced in paper I. Although

this algal cell has been extensively studied in measurements using the pressure probe [21, 22], turgor pressure relaxations have not been recognized until now as being composed of two phases. The reason for this has been the conventional method of recording and processing the data. In the case of algal cells and especially in the case of *Chara corallina*, only a small number of points along a relaxation curve was previously included in curve fittings, so that the significance of small deviations from the simple exponential course was not recognized. In the experiments presented here, the recording of data was significantly improved either by processing the pressure probe signal directly with a computer or by digitizing the relaxation curves electronically from the chart paper.

The results of some other workers indicate that the hydraulic conductivity of the tonoplast of *Chara corallina* is so large that its influence on the relaxation may be neglected [11]. We will show here that this is not the case, but it should be noted that our results hold only if the interpretation of pressure relaxations in terms of the three-compartment model can be justified. Therefore, we will examine whether effects due to unstirred layers, solvent drag phenomena, or the pressure dependence of cell wall parameters could be responsible for one of the two components of a turgor pressure relaxation.

### Materials and Methods

#### MATERIALS

Pond water algal cells of *Chara corallina* were maintained at a temperature of 17°C in artificial pond water (APW) of the following composition (in mM): 1 NaCl, 0.1 KCl, 0.1 CaCl<sub>2</sub>, 0.1 MgCl<sub>2</sub>. The cells which originated from the laboratory of H.G.L. Coster in Sydney, Australia, were continuously illuminated by Osram

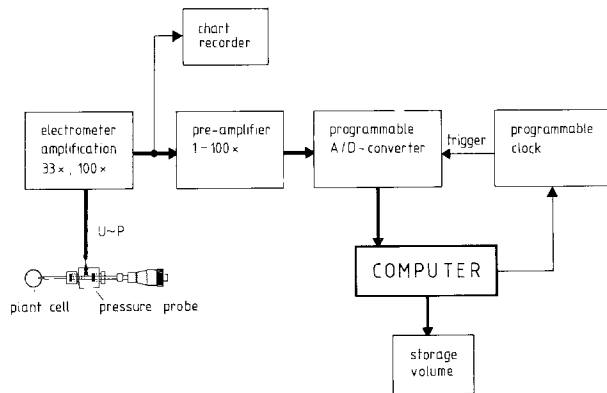


**Fig. 1.** High resolution data recording during turgor pressure relaxations. The voltage signal of the pressure probe ( $U$ ) was amplified using an electrometer and a second pre-amplifier in series. The amplified signal was converted from analog to digital at regular times and the values were stored on a mass storage volume of the computer (floppy disk). Conversion was initiated each time the counter of a programmable clock met an overflow condition at which the clock sent a trigger pulse to the A/D-converter. Thus, turgor pressure relaxations were digitized and stored for evaluation at a later time. In parallel to the computer-controlled data recording, the output of the electrometer was monitored on a chart recorder in the conventional way

Fluora lamps. For most of the experiments, single internodal cells with volumes between 5 and 32  $\mu\text{l}$  were used; in some cases lateral cells were also taken for measurements. The cell volume corresponded approximately to the volume of a cylinder whose dimensions were given by the length and mean diameter of the cells. While the length of the cells varied considerably, the cell diameter was usually 0.9 to 1.0 mm. For the purpose of comparison, some measurements were also carried out on *Chara corallina* cells originating from the laboratory of M. Tazawa in Tokyo, Japan.

## METHODS

### Data Recording and Evaluation

The use of the pressure probe to measure turgor pressure, pressure relaxations, and the volumetric elastic modulus of the cell has been described previously [17–20, 23]. During the measurement of pressure relaxations, the voltage signal of the pressure probe was sent directly to a computer (MINC 11/03, Digital Equipment Corporation, Cologne) by way of an electrometer, a pre-amplifier and a programmable analogue-to-digital converter (Fig. 1). By including the pre-amplifier with a variable amplification factor of 1 to 100 $\times$  and an offset-compensation, it was possible to amplify the output of the pressure probe up to 10,000-fold. The maximum data recording rate was 50 values per second. By choosing multiples of 20 msec as the length of the sampling interval, it was possible to eliminate unwanted coupling of the power line fundamental, as the measured values were always recorded at comparable positions of the 50-Hz waveform. For most relaxation studies of *C. corallina*, a data recording rate of 10 values per second was sufficient. Thus, up to 500 values were available for the analysis of a relaxation curve. A similar density of data

points was achieved when the curves on the chart were digitized using a Bitpad One digitizer (Kontron, Düsseldorf, W. Germany).

The relaxation curves were analyzed with the aid of computer programs which initially gave a semilogarithmic plot of the values  $|P - P_o|$  on the display terminal (cf. Fig. 4). With the aid of these graphics, it was possible to distinguish between simple exponential relaxations and relaxations consisting of two components. The measured values of single-phase relaxations were fitted to a single exponential function by the method of least squares, while relaxations with two phases were best described by a function consisting of two superimposed exponentials. For this purpose, the linear part of the semilogarithmic plot at the end of the relaxation was first fitted to an exponential function. When this curve had been subtracted from the set of data, the best-fit exponential function for the remaining values was then determined by the same procedure. All fits could be carried out with or without weighting. For most measurements, a weighted fit seemed more sensible, since those points with a low relative error, i.e. at the onset of a relaxation, were given more consideration than the values with a large relative error, i.e. towards the end of a relaxation. From the half-times and initial amplitudes of the relaxations, the hydraulic conductivities of the plasmalemma and the tonoplast, and the cytoplasmic volume were evaluated using Eqs. (1) to (3). These equations have been derived in paper I and are repeated here for reference. Solutes were assumed to be impermeable for those membranes.

$$Lp_p = \frac{V_o}{\varepsilon \cdot A_p} q \quad (1)$$

$$Lp_t = - \frac{V_2 \cdot V_3}{A_t \cdot \pi_o} \cdot V_o \left\{ k_1 + k_2 + q \left( 1 + \frac{V_o}{V_2} z \right) \right\} \quad (2)$$

$$\frac{V_2}{V_o} = - \frac{q^2 \cdot z(1+z)}{\{q^2 + (k_1 + k_2) \cdot q\}(1+z) + k_1 \cdot k_2} \quad (3)$$

with

$$z = \frac{\pi_o}{\varepsilon} \quad (4)$$

and

$$q = \frac{\alpha_1 k_1 + \alpha_2 k_2}{P_o - P_i} \quad (5)$$

where  $V_o$  = cell volume,  $V_2$  = volume of the cytoplasm,  $V_3$  = volume of the vacuole ( $V_3 = V_o - V_2$ ),  $A_p, A_t$  = exchange area of the plasmalemma/tonoplast,  $\varepsilon$  = volumetric elastic modulus of the cell wall,  $Lp_p, Lp_t$  = hydraulic conductivity of the plasmalemma/tonoplast,  $\pi_o$  = osmotic pressure of the solutes in the cytoplasm and vacuole at steady state before relaxation,  $P_o$  = turgor pressure at steady state before relaxation,  $P_i$  = turgor pressure at  $t = 0$ , i.e. the peak value of the relaxation,  $P_e$  = turgor pressure in the steady state after relaxation,  $\alpha_1, \alpha_2$  = amplitude of the fast/slow component of the relaxation and  $k_1, k_2$  = exponent of the fast/slow component of the relaxation.

### Preparation of Isolated Cell Wall Envelopes from *Chara corallina*

Isolated cell walls of *C. corallina* were obtained as follows [8, 22]: End pieces with a length of 7 to 12 mm were cut off from

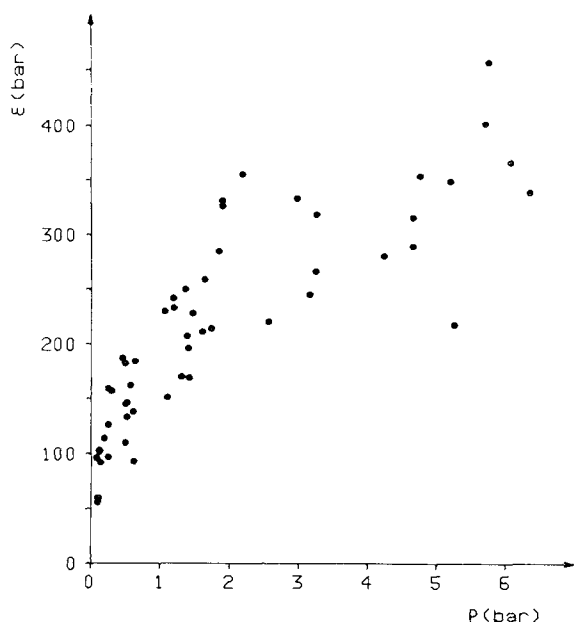


Fig. 2. Volumetric elastic modulus  $\varepsilon$  of *Chara corallina*, measured for various cells at different turgor pressures

internodal cells and flushed several times, first with distilled water, then with ethanol with the aid of a fine glass capillary. The cell wall tubes were then filled with a solution containing about 20 mM of polyethylene glycol (PEG 1000 or PEG 6000), and connected to a pressure probe. The capillary of the probe was inserted deeply into the open end of the cell wall tube which then adhered tightly to the glass. The site of contact between the capillary and the cell wall was dried by dabbing with a tissue soaked in acetone, and a pressure-tight seal was made using a mixture of bees wax and colophony. By immersing the envelope in distilled water, an osmotic gradient was set up across the cell wall which drove an inwardly directed water flow. Thus a small hydrostatic pressure (0.1 to 0.8 bar) could be established in the cell-wall tube which corresponded to a low turgor pressure in living cells. The gradual diffusion of PEG out of the tube made the pressure decline gradually. However, the rate of pressure loss was so small ( $< 5 \times 10^{-4}$  bar  $\text{sec}^{-1}$ ) that the steady-state turgor pressure could be regarded as constant for the duration of a pressure relaxation ( $T_{1/2} = 0.4$  to 1.8 sec).

In order to investigate the viscoelastic properties of cell walls, cell wall tubes with a length of 15 to 28 mm were completely filled with mercury and connected to the pressure probe as described above. In this case, however, the capillary of the pressure probe also contained mercury. Using this technique it was possible to build up and to vary turgor pressure without causing water or solute flow through the cell wall.

## Results

### DOUBLE-EXPONENTIAL PRESSURE RELAXATIONS IN *CHARA CORALLINA*

Cells of *C. corallina* showed a steady-state turgor pressure between 5 and 6.5 bar. As the osmotic

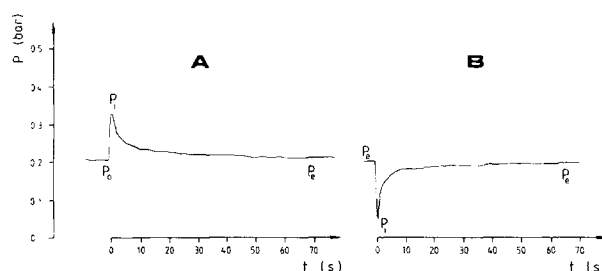


Fig. 3. Hydrostatically induced turgor-pressure relaxations in *Chara corallina* with exosmotic (A) and endosmotic (B) water flow. A cell turgor of  $P_0 = 0.21$  bar was achieved by addition of sorbitol to the external medium (artificial pond water). Cell data:  $V_o = 24 \mu\text{l}$ ,  $A_p = 121 \text{ mm}^2$ ,  $\varepsilon = 145 \text{ bar}$ ,  $\pi_o = 4.19 \text{ bar}$

pressure of the APW was close to zero (0.025 to 0.05 bar  $\pm 1$  to 2 mosmol/kg), the osmotic pressure of the cell sap was equal to the turgor pressure. For the volumetric elastic modulus of the cell  $\varepsilon$ , values between 300 and 450 bar were measured in APW. When the turgor pressure was lowered by adding sorbitol to the APW,  $\varepsilon$  decreased significantly. The pressure dependence of  $\varepsilon$  is demonstrated in Fig. 2 which summarizes the measurements for various *Chara* cells. Our results are in good agreement with earlier results for *Chara intermedia* and *Chara fragilis* obtained using the pressure probe technique [22]. However, it should be mentioned that the  $\varepsilon$  values reported by Dainty et al. [5] are about twice as high as those reported here.

Generally, turgor pressure relaxations in *C. corallina* could not be described by a single exponential function. The curves were best characterized by the sum of two exponential functions regardless of the direction of the induced water flow. This splitting of the relaxation into a fast and a slow component became more pronounced at lower cell turgors. Figure 3 shows two hydrostatically induced turgor pressure relaxations in a cell of *C. corallina*. The first curve represents an exosmotic experiment with outwardly directed water flow, and the second is an endosmotic experiment with inwardly directed water flow. The turgor pressure of the cell had previously been lowered to 0.21 bar by the addition of sorbitol to the APW. From the cell dimensions the volume of the cell was calculated to be  $24 \mu\text{l}$ , and its surface area  $121 \text{ mm}^2$  (cf. Table, cell 15). The osmotic pressure of the cell sap was 4.19 bar, calculated from the osmotic pressure of the external solution and the turgor pressure of the cell. At the given turgor pressure, the cell had an  $\varepsilon$  value of 145 bar.

Figures 4A and 4B show semilogarithmic plots of the relaxation curves of Fig. 3. Two phases can be clearly distinguished. On subtracting the slow component from the whole data set, the remaining values were fitted to a second exponential function.

For the exosmotic experiment, the slow component had an amplitude of 35 mbar and a half-time of 16 sec, whereas the fast component had an amplitude of 85 mbar and a half-time of 1.8 sec. The corre-

sponding data for the endosmotic experiment were 27 mbar and 18.6 sec for the amplitude and half-time of the slow component, respectively, and 102 mbar and 1.3 sec for the amplitude and half-time of the

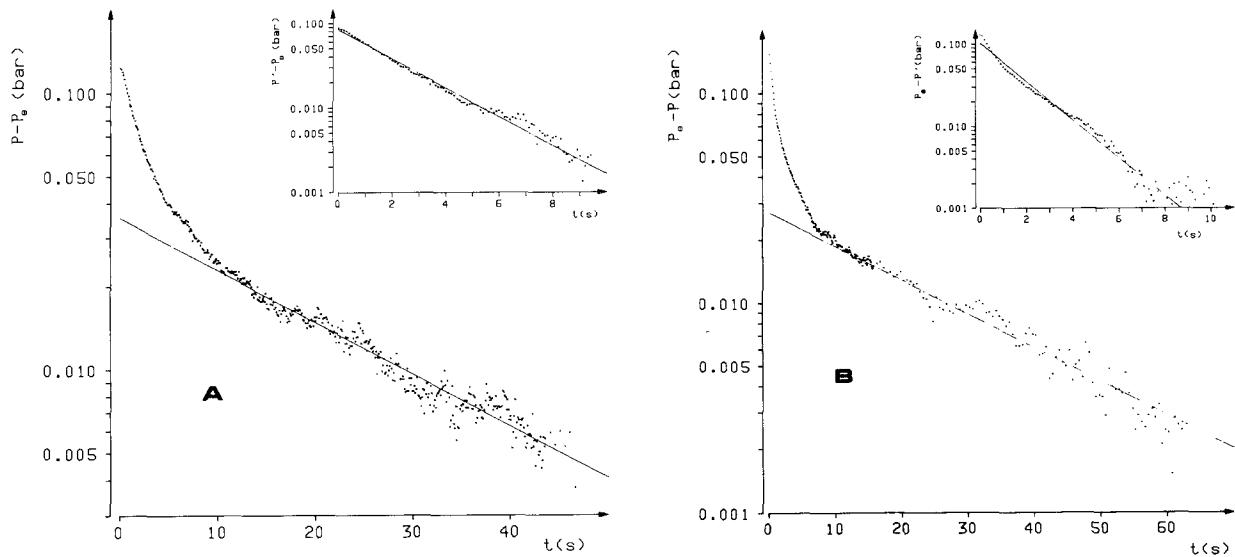


**Fig. 4.** Semilogarithmic plots of the turgor pressure relaxations shown in Fig. 3. Two phases are clearly distinguishable for both the exosmotic (A) and endosmotic (B) experiment. After subtraction of the slow component, a second exponential function could be fitted to the remaining values (insets). Results for A: amplitudes of 35 and 85 mbar, and half-times of 16 and 1.6 sec for the slow and fast component, respectively. Results for B: amplitudes of 27 and 102 mbar, and half-times of 18.6 and 1.3 sec for the slow and fast component, respectively. An evaluation on the basis of the three-compartment model gave  $3.8 \times 10^{-5} \text{ cm sec}^{-1} \text{ bar}^{-1}$  for the hydraulic conductivity of the plasmalemma and  $2.3 \times 10^{-5} \text{ cm sec}^{-1} \text{ bar}^{-1}$  for that of the tonoplast in A, and  $5.7 \times 10^{-5} \text{ cm sec}^{-1} \text{ bar}^{-1}$  for the hydraulic conductivity of the plasmalemma and  $2.4 \times 10^{-5} \text{ cm sec}^{-1} \text{ bar}^{-1}$  for that of the tonoplast in B. The cytoplasm was found to occupy 8.0% of the total volume in A and 10.5% in B. Assumptions:  $\sigma_p = \sigma_t = 1.0$   $A_t = 109 \text{ mm}^2 = 0.9 \cdot A_p$

**Table.** Calculated water relation parameters of the individual membranes<sup>a</sup>

Cell no.	$V_o$ ( $\mu\text{l}$ )	$A_p$ ( $\text{mm}^2$ )	Pressure range (bar)	$Lp_p \cdot 10^5$ ( $\text{cm sec}^{-1} \text{ bar}^{-1}$ )	$Lp_t \cdot 10^5$ ( $\text{cm sec}^{-1} \text{ bar}^{-1}$ )	$V_2/V_o$ (%)	Number of experiments
6	17	73	$P_o > 0.4$	$2.1 \pm 0.6$	$3.4 \pm 0.7$	$9.1 \pm 6.3$	13
			$< 0.2$	$5.8 \pm 1.9$	$4.5 \pm 2.2$	$9.0 \pm 5.6$	7
7	23	93	$P_o > 0.4$	$1.7 \pm 0.3$	$4.6 \pm 1.9$	$8.4 \pm 3.1$	12
			$\approx 0.0$	$6.6 \pm 0.5$	$13.5 \pm 2.0$	$14.8 \pm 4.7$	5
8	6	27	$P_o > 0.1$	$2.0 \pm 0.8$	$3.3 \pm 1.3$	$5.5 \pm 2.3$	13
11	33	121	$P_o > 1.0$	$2.4 \pm 0.2$	$9.2 \pm 3.1$	$6.1 \pm 4.3$	7
12	22	85	$P_o > 0.1$	$4.3 \pm 2.4$	$5.4 \pm 3.3$	$8.2 \pm 4.4$	21
14	20	77	$P_o > 0.1$	$3.7 \pm 1.3$	$3.9 \pm 2.6$	$10.9 \pm 4.9$	10
15 <sup>b</sup>	24	121	$P_o > 2.5$	$2.7 \pm 0.2$	$10.4 \pm 0.9$	$7.1 \pm 0.5$	4
			$< 0.25$	$4.2 \pm 0.8$	$2.6 \pm 0.5$	$9.5 \pm 2.7$	7
16 <sup>c</sup>	5	45	$P_o \approx 0.6$	$3.9 \pm 0.6$	$5.3 \pm 0.7$	$20.2 \pm 6.8$	4
17 <sup>c</sup>	4	31	$P_o = 0.16$	2.3	3.3	13.9	1

<sup>a</sup> Hydraulic conductivity of the plasmalemma ( $Lp_p$ ) and tonoplast ( $Lp_t$ ) as well as relative cytoplasmic volume ( $V_2/V_o$ ), calculated from hydrostatically induced turgor pressure relaxations in *Chara corallina*. Values  $\pm$  standard deviation.  $V_o$  = cell volume,  $A_p$  = surface area of plasmalemma,  $P_o$  = turgor pressure before relaxation. It is assumed that the surface area of the tonoplast is equal to 90% of  $A_p$ , and that the plasmalemma and tonoplast are perfectly semipermeable.

<sup>b</sup> Cell tied off at both ends.

<sup>c</sup> Cell from the laboratory of M. Tazawa, Tokyo, Japan; cell tied off at both ends.

fast component, respectively. When these experimental findings were interpreted in terms of the three-compartment model presented in paper I, the hydraulic conductivities of the plasmalemma ( $Lp_p$ ) and the tonoplast ( $Lp_t$ ), and the cytoplasmic volume relative to the total cell volume ( $V_2/V_o$ ) could be obtained. Using Eqs. (1) to (3), the curves of Figs. 4A and 4B yield the following results:  $Lp_p = 3.8 \times 10^{-5} \text{ cm sec}^{-1} \text{ bar}^{-1}$ ,  $Lp_t = 2.3 \times 10^{-5} \text{ cm sec}^{-1} \text{ bar}^{-1}$ , and  $V_2/V_o = 8.0\%$  for the exosmotic experiment (Fig. 4A), and  $Lp_p = 5.7 \times 10^{-5} \text{ cm sec}^{-1} \text{ bar}^{-1}$ ,  $Lp_t = 2.4 \times 10^{-5} \text{ cm sec}^{-1} \text{ bar}^{-1}$ , and  $V_2/V_o = 10.5\%$  for the endosmotic experiment (Fig. 4B).

In paper I, it was pointed out that  $Lp_t$  could only be estimated if assumptions regarding the reflection coefficient ( $\sigma_t$ ) and the surface area of the tonoplast ( $A_t$ ) were made, because these parameters cannot be measured independently of each other. For the calculations above  $\sigma_t$  was assumed to be 1, and  $A_t$  was made equal to 90% of the surface area of the plasmalemma, according to the large volume of the vacuole. Furthermore, the plasmalemma was assumed to be practically impermeable to solutes.

The Table summarizes the results of pressure probe measurements on 9 cells. The pressure relaxations were induced hydrostatically, i.e. by a sudden change in cell turgor pressure, and evaluated according to Eqs. (1) to (3) with the above-mentioned assumptions for  $\sigma_t$  and  $A_t$ . For turgor pressures higher than 0.4 bar, the values for the hydraulic conductivity of the plasmalemma were found to be in the range between  $2 \times 10^{-5}$  and  $4 \times 10^{-5} \text{ cm sec}^{-1} \text{ bar}^{-1}$ , whereas those for the tonoplast varied between  $3 \times 10^{-5}$  and  $1 \times 10^{-4} \text{ cm sec}^{-1} \text{ bar}^{-1}$ . The mean contribution of the cytoplasmic compartment to the cell volume was calculated to be 9%, which is in agreement with the general assumption that the

cytoplasm occupies only a thin layer between the plasmalemma and the tonoplast.

Figure 5 is a graphic representation of the  $Lp_p$  values and  $Lp_t$  values from the individual cell measurements, whose mean values are given in the Table. It is apparent from Fig. 5A that in some cells the hydraulic conductivity of the plasmalemma increases by a factor of 2 to 3 when the plasmolytic point is approached ( $P_o < 0.4$  bar) as reported elsewhere for measurements of  $Lp$  values of the total membrane barrier [21]. For turgor pressure values less than 0.4 bar, most of the  $Lp_t$  values of the tonoplast cluster around  $2.5 \times 10^{-5} \text{ cm sec}^{-1} \text{ bar}^{-1}$  (Fig. 5B). However, the accurate dependence of  $Lp_t$  on  $P$  cannot be determined from Fig. 5B because of the wide scatter of the individual  $Lp_t$  values.

#### MEASUREMENTS ON CELL WALLS OF *CHARA CORALLINA*

When interpreting the results of measurements presented here in terms of the three-compartment model, the values of the hydraulic conductivity of the plasmalemma ( $Lp_p$ ) ( $2 \times 10^{-5}$  to  $4 \times 10^{-5} \text{ cm sec}^{-1} \text{ bar}^{-1}$ ) are found to be close to the hydraulic conductivity of the cell wall of *Nitella* ( $5 \times 10^{-5}$  to  $9 \times 10^{-5} \text{ cm sec}^{-1} \text{ bar}^{-1}$  [8, 16, 22]). Since the authors cited used the method of transcellular osmosis [8] and stationary flow measurements [16, 22], an attempt was made here to determine the water permeability of the cell wall from pressure relaxations. When isolated cell wall tubes had been filled with PEG solution and connected to the capillary of the pressure probe by a pressure-tight seal, pressure relaxations were induced at internal pressures of 0.1 to 0.5 bar. The pressure relaxations showed only a single component with half-times of 0.4 to 1.8 sec.

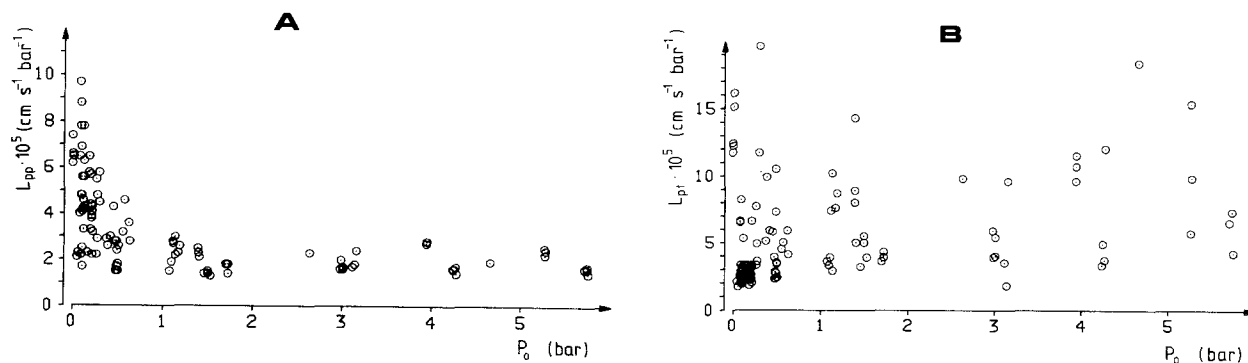


**Fig. 5.** Hydraulic conductivity of the plasmalemma  $Lp_p$  (A) and the tonoplast  $Lp_t$  (B) as a function of cell turgor  $P_o$ , determined in *Chara corallina*. The pressure increments at the beginning of relaxation were about 0.5 bar in the upper turgor range and about 0.2 bar in the lower range.  $Lp_p$  is clearly pressure-dependent (A), whereas the general scatter of  $Lp_t$  (B) does not allow one to make a similar statement for the hydraulic conductivity of the tonoplast. However, in the lower pressure range the  $Lp_t$  values (B) of some cells cluster around  $2.5 \times 10^{-5} \text{ cm sec}^{-1} \text{ bar}^{-1}$ .

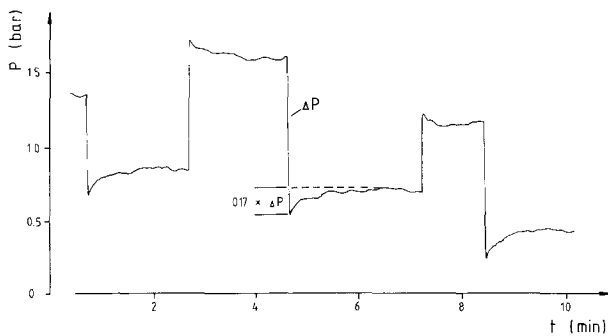


Fig. 6. Relaxation processes of mercury-filled cell walls of *Chara corallina* after pressure increments of various sizes

An evaluation according to the two-compartment model [17, 23] for the calculation of the hydraulic conductivity of the cell wall yielded  $L_p$  values between  $6 \times 10^{-5} \text{ cm sec}^{-1} \text{ bar}^{-1}$  and  $3 \times 10^{-4} \text{ cm sec}^{-1} \text{ bar}^{-1}$ . These values are higher than Tyree's values for *Nitella* ( $\approx 9 \times 10^{-5} \text{ cm sec}^{-1} \text{ bar}^{-1}$ , [16]) but are in the same range as those given by Spyropoulos [13]. Although we found that the  $L_{p_p}$  values are generally lower than the hydraulic conductivity of the cell wall, one cannot exclude the possibility that the  $L_{p_p}$  values for living cells represent the effective hydraulic conductivity of the plasmalemma/cell wall complex rather than that of the plasmalemma alone, particularly near the plasmolytic point. Furthermore, little is known about the pressure profile between the cell wall and the membrane, so that a separate consideration of the two components is not feasible.

Pressure measurements in cell wall tubes filled with mercury were performed to determine whether the viscoelastic properties of the cell wall as examined by Tazawa and Kamiya [15] could contribute to the creation of two relaxation phases. For this purpose the pressure in the cell-wall tube was increased and decreased stepwise by 0.2 to 1.8 bar as shown in Fig. 6. Immediately following a pressure step, slight relaxations were recorded in the pressure-probe/cell-wall system. These relaxations could only be of a viscoelastic nature, since the mercury filling precluded a pressure drop by volume loss. These viscoelastic wall relaxations, which often occurred in two stages and thus did not exhibit an exponential time-course, reduced the initial pressure increment  $\Delta P$  by  $18 \pm 7\%$  (53 measurements on 3 cell walls). After a time interval of  $9 \pm 5$  sec, wall relaxations had declined to half of their initial amplitude ( $\approx 5$  to  $13\%$  of the pressure increment). This "half-time" was thus considerably longer than the half-time of the rapid phase of the biphasic relaxations in living cells (1 to 3 sec). A similar test with the tip of the pressure probe capil-

lary sealed showed that the relaxation behavior observed on cell wall tubes was caused mainly by a deformation of the cell wall and to a lesser extent, by a deformation of the seals in the measuring apparatus.

## Discussion

The results presented here show that turgor pressure relaxations measured on the fresh water alga *C. corallina* could be separated into a fast and a slow exponential component. An improvement in the experimental design resulted in a high resolution of the relaxation curves, and enabled us to detect and separate the two components. Due to the poor resolution of former pressure probe measurements, turgor pressure relaxations were not recognized as composite functions until now. We have interpreted our results in the light of the three-compartment model presented in paper I. This model attributes the two relaxation components to the presence of the tonoplast which divides the cell interior into cytoplasm and vacuole. The following discussion justifies this interpretation by excluding other effects that might explain the two components of pressure relaxations.

If the hydraulic conductivity of the tonoplast in addition to that of the plasmalemma were not the reason for the two components in a turgor pressure relaxation, biphasic relaxation curves could be attributed only to processes which directly or indirectly influence water flow across the plasmalemma and the cell wall. The effects of unstirred layers or solvent drag must be considered in this context. In addition, nonlinear properties of the plasmalemma itself could also be responsible for the phenomena. Since changes of turgor pressure depend on cell wall parameters, the pressure dependence of  $\epsilon$ , or even the viscoelastic properties of the cell wall must be taken into consideration as well.

The influence of unstirred layers on the determination of the hydraulic conductivity has been studied by a number of authors [1, 6, 12]. Generally, unstirred layers lead to an underestimation of  $L_p$ . According to Dainty [2], the apparent polarity of water flow seen in the transcellular osmosis experiments of Dainty and Hope [4] can also be attributed to unstirred layers. However, as will be shown by both qualitative and quantitative arguments, the occurrence of two phases during pressure relaxation cannot be explained by the presence of unstirred layers. First, the magnitude of the unstirred layer during a pressure relaxation will be estimated. The amount of water ( $\Delta V$ ) traversing the plasmalemma during relaxation is given by:

$$\Delta V = -A_p \int_0^z J_v \cdot dt \quad (6)$$

(with  $J_v$  = volume flow,  $A$  = exchange area of the plasmalemma). As turgor pressure and volume change are coupled by the elastic properties of the cell wall, Eq. (6) can be transformed into:

$$\Delta V = -A_p \int_0^z \frac{V_o}{\varepsilon \cdot A_p} \cdot \frac{dP}{dt} dt = -\frac{V_o}{\varepsilon} \int_{P_i}^{P_e} dP$$

$$\Delta V = \frac{V_o}{\varepsilon} (P_i - P_e) \quad (7)$$

(with  $V_o$  = cell volume,  $\varepsilon$  = volumetric elastic modulus,  $P_i$  = peak value of the relaxation,  $P_e$  = turgor after relaxation). Here it was assumed that  $\varepsilon$  is not a function of  $P$ . The more realistic case of a pressure dependent  $\varepsilon$  is dealt with later. The magnitude of  $\Delta V$  is estimated with the sufficient accuracy using a constant  $\varepsilon$  value in Eq. (7).

In a representative experiment with *C. coralina* at low cell turgor,  $\Delta V$  is of the order of  $0.1 \mu\text{l}$ . The estimation was performed using typical cell parameters ( $V_o = 20 \mu\text{l}$ ,  $A_p = 80 \text{ mm}^2$ ,  $\varepsilon = 100 \text{ bar}$ ,  $P_i - P_e = 0.5 \text{ bar}$ ). If one imagines this amount of water evenly distributed in a thin layer on one side of the membrane, a value of  $1.25 \mu\text{m}$  is obtained for the thickness. We will regard this as the upper limit for the thickness of an unstirred layer that might develop during pressure relaxation. The relative change in concentration at the membrane surface can be calculated from the water flow  $J_v$ , the thickness of the unstirred layer  $\delta$ , and the diffusion coefficient  $D$  due to  $J_v \cdot \delta/D$  [7]. For  $J_v$ , the volume flow at the onset of relaxation is chosen; this was rarely larger than  $1 \times 10^{-4} \text{ cm sec}^{-1}$  in our experiments.  $D$  is assumed to have a value of  $5 \times 10^{-6} \text{ cm}^2 \text{ sec}^{-1}$  (sucrose). With these figures, a value of 0.0025 is obtained for the relative change in concentration at the membrane surface. The maximum change in the driving force caused by the formation of unstirred layers on both sides of the membrane should thus be less than 0.5%. This is too small to explain relaxation components with amplitudes of 40 to 60% of the initiating pressure step.

In addition, the effect of unstirred layers would be greatest at the beginning of a relaxation when water flow has its maximum value. This would result in a diminution of the theoretically calculated driving force ( $P - \Delta\pi$ ). To create a rapid initial phase, however, ( $P - \Delta\pi$ ) must be larger than the theoretical value. This qualitative argument also explains why unstirred layers cannot be responsible for the observed shape of curve.

Solvent drag effects were examined theoretic-

cally by using the computer program described in Appendix B of paper I. The coupled equations for volume flow and solute flow across the plasmalemma (Eqs. (B1) and (B2) of the cited paper) were solved numerically in the case where the solvent-drag term did not vanish. In a number of calculations, the membrane permeability  $P_s$  was set to zero in order to separate the solvent-drag effect from diffusional-flow effects. Pressure relaxations were calculated this way for various reflection coefficients. A semilogarithmic plot of these relaxation curves showed straight lines in all cases. The simple exponential character was retained even when the reflection coefficient was small ( $\sigma_p = 0.1$ ), i.e. when flow coupling was high. These findings exclude solvent drag as a cause of the observed shape of experimental relaxation curves. Additional calculations considered solvent drag and diffusional flow across the plasmalemma simultaneously ( $\sigma_p < 1$  and  $P_s \neq 0$ ). In reality, a nonvanishing permeability of the plasma membrane would lead to a gradual decline in turgor pressure unless it is compensated by an active solute uptake or by a continuous regeneration of osmotic pressure inside the cell. Therefore, a constant solute influx was assumed in the calculations which compensated the diffusional flow out of the cell at steady-state turgor pressure. Various combinations of  $\sigma_p$ ,  $P_s$  and  $J_a$  produced deviations from the simple exponential character of a turgor relaxation. However, no combination matched the experimental result. Therefore, we concluded that our experimental observations cannot be explained in terms of solute-flow effects at the plasmalemma.

Kedem and Katchalsky [10] proposed a model which describes a single membrane as a double-membrane system with the space between the partial membranes filled with solute. Suppose that the plasma membrane of *C. corallina* had the characteristics of such a double-layer system, but that the two layers had different reflection coefficients. Deviations from the exponential character of a relaxation would be possible, because the relationship between  $J_v$  and the driving force would no longer be linear [10]. However, in this case, one would expect a marked polarity of the water flows [7], so that the rapid component either for endosmotic or for exosmotic water flow should vanish. This is in contrast to our observation and to the experimental results of Steudle and Tyerman [14].

Since we have seen that transport processes at the plasmalemma are unlikely to be the cause of two-component relaxations, the cell wall properties will now be considered. The elasticity of cell walls is pressure dependent in many cells ([17, 21, 23]; see also Fig. 2). The question is, can the pressure dependence of the volumetric elastic modulus cause two components in a turgor pressure relaxation?

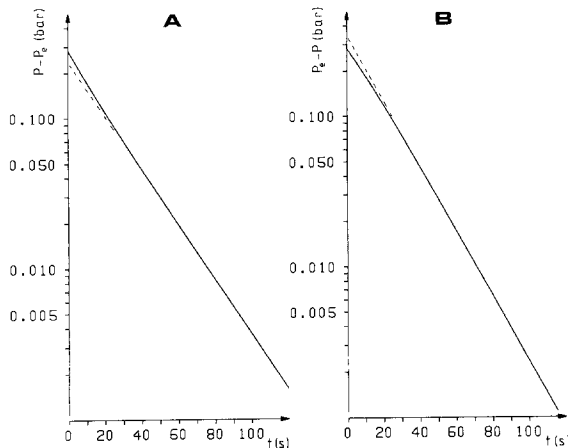


**Fig. 7.** Numerically calculated turgor pressure relaxations in the pressure range between 0.2 and 0.5 bar for exosmotic (A) and endosmotic water flow (B). The calculations were carried out on the basis of the two-compartment model with pressure-dependent  $\varepsilon$ . The cell data used are typical of *Chara corallina*:  $V_o = 25 \mu\text{l}$ ,  $A_p = 100 \text{ mm}^2$ ,  $Lp = 1 \times 10^{-5} \text{ cm sec}^{-1} \text{ bar}^{-1}$ ,  $\pi_o = 6 \text{ bar}$ ; A:  $P_o = 0.2 \text{ bar}$ ,  $P_i = 0.5 \text{ bar}$ ; B:  $P_o = 0.5 \text{ bar}$ ,  $P_i = 0.2 \text{ bar}$ . In the turgor pressure range studied, the pressure dependence of  $\varepsilon$  was approximately linear with  $\varepsilon = 80 \cdot P + 80 \text{ bar}$  (cf. Fig. 2). The first part of both relaxation curves lies above or below the linearly extrapolated final part (dashed lines), the deviations being of the order of +17% (A) and -13% (B), respectively, of the initial amplitude  $|P_i - P_o|$ .

Numerically calculated pressure relaxations give an answer to this question. Again, the computer program mentioned in paper I was used to solve the differential equation for water flow assuming for simplicity that the volumetric elastic modulus was linearly dependent on turgor pressure in the pressure range of the considered relaxations. Figure 7 shows the result for an exosmotic (Fig. 7A) and an endosmotic pressure relaxation (Fig. 7B), i.e. for water flow after a positive and a negative pressure increment. The cell parameters that were used in the calculations are those of a typical *Chara* cell and are given in the figure legend. In Fig. 7, the linear part of each relaxation was extrapolated to the start of the hypothetical experiment at  $t = 0$  (dashed lines). Note that the endosmotic curve initially runs below the linear extrapolation of its final part (Fig. 7B). This is contradictory to the experimental finding (Fig. 4B).

The two components of a relaxation curve could in principle arise if the rapid one was caused not by water flow but by the viscoelastic deformation of the cell wall and the associated volume change. In this case, the positive pressure step which initiates a pressure relaxation would bring about an increase in cell volume by displacements in the fibrillar network of the cell wall resulting in a

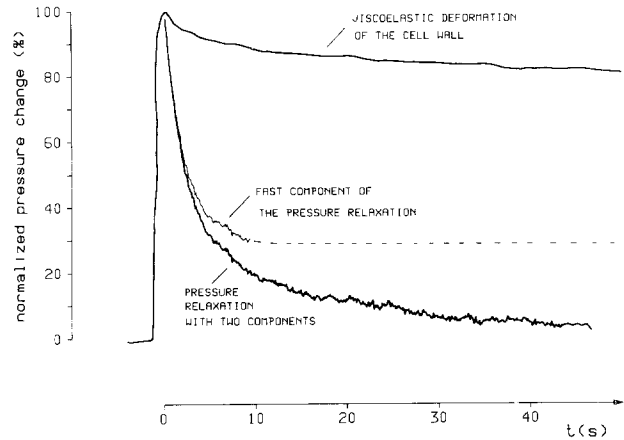


**Fig. 8.** Cell wall relaxation due to viscoelastic deformation, in comparison to a pressure relaxation and its fast component in *Chara corallina*. The fast component of a pressure relaxation cannot be explained by the viscoelastic properties of the cell wall. Note the difference in the amplitudes and half-times of the two phenomena

rapid component at the beginning of the turgor pressure relaxation. When the pressure increment was negative, the cell wall would have to contract a little in order to induce a rapid initial phase under these conditions. This behavior of the cell wall was in fact observed qualitatively in experiments on cell wall tubes filled with mercury (see the preceding chapter). Similar viscoelastic properties are also known from cell walls of *Nitella flexilis* [9]. However, in the case of a wall relaxation occurring after a pressure increment  $\Delta P$ , the mean amplitude of 18% was too small, and the mean half-time of 9 sec too large to explain the existence of the rapid component (50 to 70%, 1 to 3 sec). In Fig. 8, a typical pressure relaxation and its fast component are compared to the viscoelastic relaxation of a cell wall tube to illustrate the dissimilarity of the two phenomena. The slow component cannot be attributed to cell wall deformation, because the water flow then represented by the fast component would lead to complete relaxation of the pressure increment within a few seconds. Thus, the driving force for cell wall deformation would also vanish. Actually this effect must be borne in mind because the pressure increment is in any case rapidly reduced by water flow. Therefore, the results of the wall experiments with mercury represent the worst case, in which the driving force for the wall deformation is maintained longer than during a pressure relaxation.

It has been shown that influences of unstirred layers, solvent drag phenomena, and nonlinear properties of the plasmalemma are unlikely explanations for the experimental findings. Cell wall ef-



fects are also too small to be responsible for the fast component of a pressure relaxation. Since none of the preceding considerations have provided a satisfactory explanation for the occurrence of two relaxation components, it seems sensible to evaluate the curves on the basis of the three-compartment model. In our opinion this gives a reasonable explanation of the observed pressure curves.

If one follows the hypothesis that the 'fine structure' of the relaxation curves is the result of an interaction between the water resistances of the tonoplast and plasmalemma, we obtain the following information. The hydraulic conductivity of the plasmalemma ( $Lp_p$ ) was  $2 \times 10^{-5}$  to  $4 \times 10^{-5}$  cm sec $^{-1}$  bar $^{-1}$  for turgor pressure values larger than 0.4 bar. This is almost twice as large as the  $Lp$  values published earlier [3–5, 15, 22]. Note that this discrepancy is at least partially a direct consequence of the different interpretation of the relaxation curves (two-compartment model *versus* three-compartment model). In the lower pressure range with turgor pressure less than 0.4 bar, an increase of  $Lp_p$  by a factor of 2 to 3 was observed in most of the cells. This is in agreement with earlier measurements with the pressure probe, when  $Lp$  was attributed to the whole membrane barrier system [17–19, 23]. The hydraulic conductivity of the tonoplast ( $Lp_t$ ) was  $3 \times 10^{-5}$  to  $1 \times 10^{-4}$  cm sec $^{-1}$  bar $^{-1}$ . For turgor pressures greater than 0.4 bar,  $Lp_t$  was larger than  $Lp_p$ . The reverse seems to be true near the plasmolytic point for turgor pressures less than 0.4 bar. In this pressure range,  $Lp_t$  values cluster around  $2.5 \times 10^{-5}$  cm sec $^{-1}$  bar $^{-1}$ , whereas  $Lp_p$  values are larger by a factor of two or three. Actually, a complementary pressure dependence of  $Lp_p$  and  $Lp_t$  would explain why the two phases of turgor relaxations were more pronounced at low turgor pressures. This is illustrated in Fig. 9, which shows two pressure relaxations calculated using the same set of cell parameters except for the  $Lp$  values of the tonoplast and the plasmalemma. Curve 1 represents a pressure relaxation which could have been measured at high cell turgor when  $Lp_p = 2 \times 10^{-5}$  cm sec $^{-1}$  bar $^{-1}$  and  $Lp_t = 1 \times 10^{-4}$  cm sec $^{-1}$  bar $^{-1}$ . Although the two phases can be distinguished in the theoretical curve, a separation would hardly be possible in the case of a noisy experimental relaxation. The half-times of the two components (2 and 5.1 sec) are too similar. Curve 2 could have been measured at low turgor pressure. Here,  $Lp_p = 6 \times 10^{-5}$  cm sec $^{-1}$  bar $^{-1}$  and  $Lp_t = 2 \times 10^{-5}$  cm sec $^{-1}$  bar $^{-1}$  were assumed. It is obvious that the two phases can easily be distinguished as the half-times of 0.8 and 21 sec are sufficiently different. Therefore, we conclude that the pressure dependence of  $Lp$  for both membranes is in favor of the pronounced splitting of

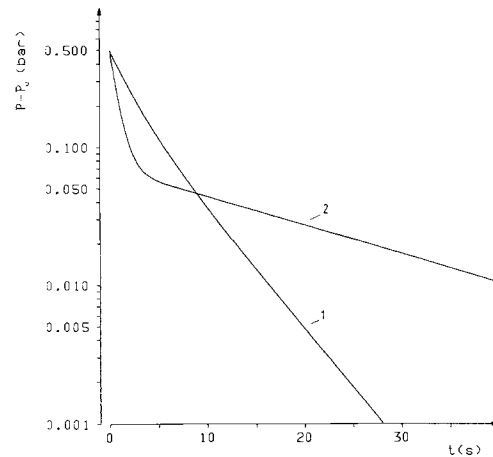


**Fig. 9.** Numerically calculated pressure relaxations in the context of the three-compartment model. Curve 1:  $Lp_p = 2 \times 10^{-5}$  cm sec $^{-1}$  bar $^{-1}$  and  $Lp_t = 1 \times 10^{-4}$  cm sec $^{-1}$  bar $^{-1}$ . Curve 2:  $Lp_p = 6 \times 10^{-5}$  cm sec $^{-1}$  bar $^{-1}$  and  $Lp_t = 2 \times 10^{-5}$  cm sec $^{-1}$  bar $^{-1}$ . The two exponential components can be more easily separated in curve 2 than in curve 1. In general, the separation is more distinct when  $Lp_p$  is high and  $Lp_t$  is low

turgor pressure relaxations in two components at low cell turgors.

The cytoplasmic volume of *C. corallina* was also calculated on the basis of the three-compartment model using Eq. (3). The mean value of 9% of the total cell volume is consistent with the large vacuoles known to exist in *Chara* cells.

We wish to thank Dr. K.-H. Büchner for stimulating discussions. His invaluable help in designing the electronic part of the measuring device is gratefully acknowledged. Furthermore, we thank Drs. W.M. Arnold, G. Pilwat and E. Steudle for critical reading of the manuscript. This work was supported by a grant (SFB 160) from the Deutsche Forschungsgemeinschaft to U.Z.

## References

1. Dainty, J. 1963. The polar permeability of plant cell membranes to water. *Protoplasma* **57**:220–228
2. Dainty, J. 1976. Water relations of plant cell. In: *Encyclopedia of Plant Physiology*. U. Lüttge and M.G. Pitman, editors. New Series, Vol. 2, pp. 12–35. Springer, Berlin-Heidelberg-New York
3. Dainty, J., Ginzburg, B.Z. 1964. The measurement of hydraulic conductivity (osmotic permeability to water) of inter-nodal Characean cells by means of transcellular osmosis. *Biochim. Biophys. Acta* **79**:102–111
4. Dainty, J., Hope, A.B. 1959. The water permeability of cells of *Chara australis*. *Aust. J. Biol. Sci.* **12**:136–145
5. Dainty, J., Vinters, H., Tyree, M.T. 1974. A study of trans-cellular osmosis and the kinetics of swelling and shrinking in cells of *Chara corallina*. In: *Membrane Transport in Plants*. U. Zimmermann and J. Dainty, editors. pp. 59–63. Springer, Berlin-Heidelberg-New York

6. Everitt, C.T., Haydon, D.A. 1969. Influence of diffusion layers during osmotic flow across bimolecular lipid membranes. *J. Theor. Biol.* **22**:9–19
7. House, C.R. 1974. Water transport in cells and tissue. Edward Arnold, London
8. Kamiya, N., Tazawa, M., Takata, T. 1962. Water permeability of the cell wall in *Nitella*. *Plant Cell Physiol.* **3**:285–292
9. Kamiya, N., Tazawa, M., Takata, T. 1963. The relation of turgor pressure to cell volume in *Nitella* with special reference to mechanical properties of the cell wall. *Protoplasma* **57**:501–521
10. Kedem, O., Katchalsky, A. 1963. Permeability of composite membranes. Part 3: Series array of elements. *Trans. Faraday Soc.* **59**:1941–1953
11. Kiyosawa, K., Tazawa, M. 1977. Hydraulic conductivity of tonoplast-free *Chara* cells. *J. Membrane Biol.* **37**:157–166
12. Kuhn, W. 1951. Grenze der Durchlässigkeit von Filtrier- und Löslichkeitsmembranen. *Z. Elektrochem.* **55**:207–217
13. Spyropoulos, C.S. 1983. Hydraulic conductivity of *Nitella* cells using the intracellular perfusion technique. *J. Membrane Biol.* **76**:17–26
14. Steudle, E., Tyerman, D.S. 1983. Determination of permeability coefficients, reflection coefficients, and hydraulic conductivity of *Chara corallina* using the pressure probe: Effects of solute concentrations. *J. Membrane Biol.* **75**:85–96
15. Tazawa, M., Kamiya, N. 1965. Water relations of characean internodal cell. *Annu. Rep. Biol. Works, Fac. Sci. Osaka Univ.* **13**:123–157
16. Tyree, M.T. 1968. Determination of transport constants of isolated *Nitella* cell walls. *Can. J. Bot.* **46**:317–327
17. Zimmermann, U. 1977. Cell turgor regulation and pressure mediated transport processes. In: Integration of activity in the higher plant. D. Jennings, editor. pp. 117–154. Cambridge University Press, Cambridge
18. Zimmermann, U. 1978. Physics of turgor- and osmoregulation. *Annu. Rev. Plant Physiol.* **29**:121–148
19. Zimmermann, U. 1980. Pressure mediated osmoregulatory processes and pressure sensing mechanism. In: Animals and Environmental Fitness. R. Gilles, editor. pp. 441–459. Pergamon, Oxford
20. Zimmermann, U., Råde, H., Steudle, E. 1969. Kontinuierliche Druckmessung in Pflanzenzellen. *Naturwissenschaften* **56**:634–635
21. Zimmermann, U., Steudle, E. 1974. Hydraulic conductivity and volumetric elastic modulus in giant algal cells: Pressure and volume dependence. In: Membrane Transport in Plants. U. Zimmermann and J. Dainty, editors. pp. 64–71. Springer, Berlin-Heidelberg-New York
22. Zimmermann, U., Steudle, E. 1975. The hydraulic conductivity and volumetric elastic modulus of cells and isolated cell walls of *Nitella* and *Chara* spp.: Pressure and volume effects. *Aust. J. Plant Physiol.* **2**:1–12
23. Zimmermann, U., Steudle, E. 1978. Physical aspects of water relations of plant cells. *Adv. Bot. Res.* **6**:45–117

Received 7 August 1984; revised 2 January 1985